

DEPARTMENT OF THE INTERIOR

U.S. GEOLOGICAL SURVEY

Paleomagnetic and rock magnetic study of  
16,000 to 49,000 year-old wet lake sediments,  
Walker Lake, northern Arizona

by

Gene A. Clough<sup>1,2</sup> and Donald P. Elston<sup>1</sup>

Open-File Report 89 -152

This report is preliminary and has not been reviewed for conformity with U.S. Geological Survey editorial standards and stratigraphic nomenclature. Any use of trade names is for descriptive purposes only and does not imply endorsement by the U.S. Geological Survey.

<sup>1</sup>U.S. Geological Survey  
2255 N. Gemini Drive  
Flagstaff, Arizona 86001

<sup>2</sup>also Department of Geology  
Bates College  
Lewiston, Maine 04240

**Paleomagnetic and rock magnetic study of 16,000 to 49,000 year-old  
wet lake sediments, Walker Lake, northern Arizona**

by

Gene A. Clough and Donald P. Elston  
U.S. Geological Survey, Flagstaff, Arizona 86001

**Abstract**

A detailed rock-magnetic study has been performed on sediments ranging from 49,000 to 16,000 years of age from Walker Lake, near Flagstaff, Arizona. Magnetic intensity and initial susceptibility data collected from two five-meter-thick sections, separated horizontally by four meters, correlate well. The upper limit of magnetic particle size is near 1  $\mu\text{m}$ . Changes in intensity of magnetization are related mainly to changes in magnetic mineralogy, and no paleointensity record of the earth's field could be extracted from the data. The magnetic directions have an average inclination significantly shallower than would be predicted for an axial dipole. High-resolution correlations of declination and inclination data between sections are poor and no stratigraphically reproducible geomagnetic secular variation record was obtained. The paths of the virtual geomagnetic poles (VGP) do not circle the geographic pole, but rather, describe wandering "far side" traces.

**INTRODUCTION**

A 5 m-thick sequence of compact, laminated to thinly-bedded, wet lake sediments at Walker Lake, northern Arizona, made accessible through excavation rather than coring, has been the subject of a multidisciplinary study (Adam and others, 1985). We present here the results of paleomagnetic and rock-magnetic studies of two five-meter-thick sections that were sampled to investigate stratigraphic reproducibility of magnetization from virtually continuous records. The methods of Banerjee and others (1981), King and others (1982), and King and others (1983) were employed to assess the magnetic composition and grain size of the sediments, and to evaluate their suitability for relative paleointensity studies. We also investigated the validity of using anhysteretic remanent magnetization (ARM) as a normalizing factor for evaluating paleointensity, as discussed by Levi and Banerjee (1976), and we present limited observations on the anisotropy of magnetic susceptibility of these sediments. Finally, we discuss the character of the apparent geomagnetic secular variation

record contained in the sediments, and contrast the polar paths obtained from the two sampled sections.

## GEOLOGIC SETTING AND PREVIOUS WORK

Walker Lake, of Pleistocene and Holocene age, occupies part of the crater floor of a small (~800 meter diameter) basaltic cinder cone located about 23 km northwest of Flagstaff, Arizona (Figure 1). The cone is part of the extensive San Francisco volcanic field, first described in detail by Robinson (1913). Verbeck (1971) further studied the geology of the area that includes Walker Lake. Since 1965, Walker Lake has been the site of occasional projects (mainly palynologic) of the School of Forestry at Northern Arizona University (Richard Berry, personal communication, 1977; Berry and others, 1982). Initial paleomagnetic investigation of the Walker Lake section was carried out in 1976-78 by E. Gomez of the U.S. Geological Survey, who demonstrated the stability of magnetization and the potential value of a paleomagnetic study of these wet lake sediments.

## STRATIGRAPHY

The stratigraphy and sedimentology of the Walker Lake section are summarized in Figures 2 and 3. In the locality sampled, adjacent to the south shore of the present Walker Lake, one meter of highly organic soil overlying one meter of volcanic ash and cinders covers a five-meter-thick deposit of moist clay. About 1.8 meters of pebbly colluvium underlies the clay, beneath which we found two thinner clay units separated by more colluvium. These lower clay units were sampled, but only the five-meter-thick clay deposit is discussed in this report.

Figure 2 depicts the general stratigraphy exposed in the south wall of an east-west trending pit. The distribution of two sets of monolithic "channels" in two columns, collected for paleomagnetic analysis, is shown, as are a series of samples collected for X-ray photography. The positions of a series of 10 samples collected for  $^{14}\text{C}$  dating also are shown in Figure 2. Preliminary results of the dating by Stephen W. Robinson (personal communication, 1984), are shown in Figure 3.

A generalized stratigraphic column of the 5 m-thick section of clay underlying the cover of volcanic ash and cinders is shown in Figure 3. The deposits sampled for paleomagnetic analysis consist dominantly of dark to light medium gray, massive to thin-bedded and laminated carbonaceous clay. Four units, arbitrarily designated A, B, C, and D, are recognized from base to top. Although cursory inspection might suggest that deposition was essentially continuous, there is evidence of one or more hiatuses, and several changes

in depositional environment. Two granular intervals, suggesting minor dessication, are present within and at the top of unit A, at depths of 4.004 m and 3.665 m, respectively. Radiocarbon dates straddling the boundary between units A and B at a depth of 3.665 m suggest a hiatus of perhaps 4000 years (Figure 3). Granular clay also marks the top of unit B at a depth of 2.886 m, suggesting a hiatus. The contact between units C and D, at a depth of 2.010 m, marks an abrupt change from finely laminated clay below to more coarsely laminated clay above. The contact between units C and D is planar and sharp. Radiocarbon dates above and below this contact suggest no appreciable time loss at this horizon.

## SAMPLING AND MEASUREMENT TECHNIQUES

A clamshell bucket was used to excavate a nine-meter-deep pit to the base of the section shown in Figure 2. A three-tiered wooden scaffold was constructed to allow detailed examination and sampling of the south wall. The south wall was selected to minimize problems caused by surface drying during the two weeks of field work. When the clay section was to be sampled, a fresh surface was shaved smooth and vertical grooves carved so that lengths of aluminum channel (4 cm x 13 cm x 0.4 cm, and about 61 cm long) could be pressed into the clay. The stratigraphic positions and orientations of the channels were measured, and the channels and contained clay (with supplemental protective material) were carved from the wall. The unit was wrapped in plastic film, heat-sealed in an airtight bag, and stored in a refrigerator until samples were cut and processed in the paleomagnetic laboratory. Two adjacent columns of channels were collected from the east end of the south face, and two columns of channels were collected from the west end. One set from each end was retained for archival purposes. Separation between the sampled sections was approximately four meters. Several additional channels were collected for "dress rehearsals" of laboratory techniques. About 50 channels were collected in all.

All stratigraphic positions were measured and are reported with respect to the cinders/clay contact at the top of the five-meter clay section. Because this contact is somewhat irregular, this datum was defined arbitrarily near the center of the east-west-trending, south wall of the pit.

In the laboratory, the channels were processed one at a time. A channel was unwrapped, and excess clay sliced away with a wire cutter (similar to a cheese slicer) to provide a smooth surface that was immediately photographed. The body of clay within the channel was then carved into a series of adjacent, small cubes, which were slipped snugly into cubic plastic boxes having a volume of about 7 cm<sup>3</sup>. Following this, lids were glued on the boxes. With rare exception, three contiguous samples were obtained from each horizon in a vertically continuous sampling, resulting in the centers of adjacent samples

being separated horizontally and vertically by about 2 cm. From each end of the pit, more than 260 horizons of three samples each provided a total of some 1,600 paleomagnetic samples from the five-meter clay section.

The direction and intensity of natural remanent magnetization (NRM) was measured for all samples. In addition, for one column of samples, initial susceptibility was measured along each of the three principal axes of the sample cubes employing the cryogenic magnetometer.

To explore the nature of the NRM, step-wise alternating-field demagnetization was performed on about every eighth sample from one column, or 30 samples. After examination of the results (discussed below), all samples were demagnetized in peak alternating fields of 7.5, 15, and 25 mT. An anhysteretic remanent magnetization (ARM) was induced in one column of samples, using a steady field of 0.04 mT and a peak alternating field of 90 mT; these samples were then similarly demagnetized in three steps. Essentially the same procedure was followed with samples from both ends of the pit. Seventeen samples were then selected from one column for hysteresis-parameter measurement, and five samples were selected for a study of the acquisition of isothermal remanent magnetization (IRM).

## MAGNETIC MINERALOGY

Figure 4 presents IRM acquisition curves for five samples distributed across the section. Near-saturation of three samples in fields of 0.8T suggests that magnetite is the dominant magnetic carrier. However, two samples selected from relatively high in the section (at depths of 0.606 and 1.843 m) acquired IRMs less readily than the other samples, suggesting the presence of some other additional carrier(s) of magnetization with higher coercivity.

## MAGNETIC STRATIGRAPHY

Figure 5 presents orthogonal demagnetization diagrams for four typical samples. Following study of nearly 100 of these, 7.5 mT was selected as an appropriate AF "cleaning" field for all of the samples, and all remaining samples were demagnetized with this peak field in a tumbling demagnetizer. Later, to see the effect on the overall magnetic stratigraphy, all samples also were demagnetized at 15 and 25 mT.

Figure 6 displays the magnetostratigraphic results from the east and west columns, demagnetized at 7.5 mT. While discussions of various aspects of these data are given in

sections that follow, one should note here the close agreement between the susceptibility and intensity records obtained from the two sediment columns, four meters apart. Even small-scale magnetic features are duplicated from one section to the other. A small number of rather scattered or "wild" points on the NRM intensity plots moved in to join the curve of the 7.5 mT AF demagnetization plot, validating the choice of 7.5 mT as an appropriate "cleaning" field. The intensity plots following AF demagnetization at 25 mT are considerably "noisier" than the earlier ones, suggesting that this choice of cleaning field would have been too high. However, the plot for cleaning at 15 mT is nearly indistinguishable from that for 7.5 mT, so considerable leeway existed in the choice of cleaning field. Plots of declination and inclination of magnetization do not show obvious correlation in major features between the east and west sections.

## GRANULOMETRY

Banerjee and others (1981) and King and others (1982) describe a simple method for rapidly assessing relative size ranges of magnetite grains in sediments. Briefly, initial or low-field magnetic susceptibility,  $\chi$ , is particularly sensitive to the concentration of relatively coarse grains. In contrast, the intensity of ARM is more sensitive to the presence of smaller grains. Therefore, if one plots  $\chi$  vs ARM for a group of samples, one should expect different grain size fractions to cluster around lines of different slopes. (The distance of each point from the origin is related to the amount of magnetic material.)

We present such a plot for our data (east column only--about 260 points) as Figure 7. The plot is drawn on log-log axes because of the very large range of values displayed. On a log-log plot, a linear relationship is described by a line of slope unity (i.e., one decade per decade). Two such lines have been drawn on this plot. The lower one passes through a cluster of points for which  $\chi$  is relatively large when compared with ARM, that is, those corresponding to relatively "large" grains. The upper line passes through a cluster of points for which  $\chi$  is relatively small, when compared with ARM, corresponding to "small" grains. The crude "stratigraphy" presented on this plot through use of a different symbol for each meter of section suggests the following: The magnetic grains in the section from 0 m down to about 2 m are relatively coarse, those from about 2 m down to about 4 m are relatively fine, and those below 4 m are of variable grain size, not resolved at this one-meter "resolution." The strongest justification for this approach is the work of Dankers (1978) and Özdemir and Banerjee (1982), who applied this technique to synthetic samples of known grain size. Their data were examined by King and others (1983), who found that ARM/ $\chi$  ratio varied monotonically with grain size and proposed a phenomenological model relating grain size to ARM/ $\chi$  ratio. Applying their model to the

plot of Figure 7 suggests that the relatively larger-grained fraction is dominated by magnetic particles near or larger than about  $1.0\ \mu\text{m}$  in size, whereas the relatively finer fraction mainly contains particles closer to  $0.1\ \mu\text{m}$ .

Additional information about the nature and size of the magnetic particles is available through the hysteresis method of Day and others (1977). Figure 8 displays the results of hysteresis parameter measurements on 17 samples. The same stratigraphic symbols have been used as in Figure 7. The experimental work of Day and others (1977) has shown that on such a plot a general trend with grain size is to be expected, with small single-domain grains falling in the upper left, and larger multi-domain grains in the lower right. Most (14 out of 17) of the Walker Lake samples fall into the intermediate pseudo-single-domain region of Day and others (1977, Fig. 4), though the borders of the regions are not sharply defined and, in any case, are compositionally dependent.

The absolute particle size range associated with pseudo-single-domain magnetite by Day and others (1977) is consistent with the size estimates made above from the work of King and others (1983). However, note that the stratigraphic trend of the Walker Lake samples in Figure 8 is radial with changes in grain size (grain size tends to increase with distance from the origin), that is, perpendicular to the direction associated with changes in grain size by Day and others (1977). One possible interpretation is that this reflects compositional variations.

## PALEOINTENSITY

The grain-size estimates discussed in the previous section are important if one is to attempt to identify and estimate changes in the relative paleointensity of the earth's magnetic field during accumulation of a section. The natural remanent magnetization measured in a rock or sediment sample is normally the product of a number of factors, one of which is the concentration of magnetic material. Ideally, another factor is the intensity of the earth's magnetic field at the time of formation. Much effort has gone into determining the conditions under which measured NRM would in fact be proportional to the ancient field, and the appropriate "normalizing factor" for each case.

In the case of igneous rocks, whose remanence is acquired during cooling, the method of Thellier and Thellier (1959) has been widely and successfully used. In it, the NRM is compared with laboratory-induced thermal remanent magnetization (TRM). The success of this method probably arises because the mechanism for acquisition of the remanence is essentially the same in the laboratory as in nature.

For sedimentary deposits the situation is not so clear, because the exact mechanism of acquisition of remanence is not as well understood as for the acquisition of thermal remanence. Furthermore, even if the acquisition of depositional remanence were fully

understood, reproducing the exact conditions of deposition in laboratory redeposition experiments to provide "calibration" data would remain difficult, if not impossible. Hence, alternate schemes for the normalization of NRM data for the determination of relative paleointensities for sedimentary deposits have been sought.

One seeks an easily-measured quantity whose relationship to the magnetic mineralogy of the sedimentary rocks under study is similar to that of the NRM. IRM (Johnson and others, 1948), saturation IRM (Nakajima and Kawai, 1973), weak-field susceptibility  $\chi$  (Nesbitt, 1966, and Harrison, 1966), and ARM (Johnson and others, 1975), have all been explored by those cited and by other workers. Levi and Banerjee (1976) reviewed the foregoing work and suggested some minimum criteria for selection of a normalization technique. Specifically, to ensure that the same general "spectrum" of magnetic particles is excited by both the NRM and the "candidate" normalization parameter, the normalized AF demagnetization curves of both quantities should be similar. Said in another way, the ratio NRM/(normalizer) should remain relatively constant as both of these quantities are progressively demagnetized. We now apply this criterion to our data.

Figure 9 presents normalized AF demagnetization curves of NRM, ARM, and IRM for two samples--one from the "fine" range and one from the "coarse" range. Note that the three curves for each of the samples are not the same, and that the NRM is "softer" than both the ARM and IRM over most of the range of stability for the samples. This suggests that different magnetic mineralogies dominate each curve.

These same parameters for four different samples are presented in another form (Figure 10), where the relative paleointensity "candidates," NRM/ARM and NRM/IRM, are plotted as functions of AF demagnetization level. Note that the values of these ratios are very sensitive to the choice of demagnetization level, giving little support to the use of either of these quantities as a paleointensity indicator.

Finally, Figure 11 is a plot of NRM intensity vs initial susceptibility for 260 sample horizons from the east column. These quantities are strongly correlated over the entire section in spite of the very large variations in the individual magnitudes. Because the initial susceptibility is a function only of the mineralogy and is independent of the paleointensity of the earth's field, we must conclude that the NRM intensity is also, and that the sediments at Walker Lake thus do not reflect variations in the intensity of the field.

A single major departure exists between the congruency of the NRM plots of intensity and initial susceptibility (Figure 6). It is found from the top of the sampled section downward to a depth of 0.59 m. The decrease upward in intensity, not accompanied by an

equivalent decrease in susceptibility, corresponds to an interval of alteration beneath the unconformity at the top of the clay section. The alteration, which has resulted in an irregular bleaching of an originally dark gray clay, presumably arose as a consequence of percolation of ground water through the porous ash layer overlying the clay. The alteration also has resulted in an increased scatter in declinations and inclinations measured from samples in this interval.

In an extension of work cited earlier, King and others (1983) suggest definite minimum requirements for a sediment if it is to be employed for providing an estimate of the relative paleointensity of the earth's field. First, the remanence should be carried by 1-15  $\mu\text{m}$  magnetite particles. Here, the Walker Lake samples fail. Our evidence indicates that 1  $\mu\text{m}$  is about the upper limit of magnetic particle size in the Walker Lake sediments. Secondly, the magnetite concentration should vary at most over a factor of 20-30 (to minimize the role of particle interactions). Here also the Walker Lake samples fail. If the saturation magnetization,  $J_s$ , is taken as an indication of magnetite content (a method suggested by King and others, 1983), then the values of the Walker Lake samples vary over a factor of about 55. Hence, this line of evidence also indicates that no record of fluctuations in the intensity of the earth's magnetic field has been recorded at Walker Lake.

## MAGNETIC FABRIC

Although not equipped at the time to measure the full tensor of anisotropic magnetic susceptibility, we did measure the bulk initial susceptibility along the three perpendicular axes of the sample cubes. The "z" directions were within a few degrees of vertical, and thus nearly perpendicular to bedding, and the "x" and "y" directions were within a few degrees of lying in the plane of the bedding. If  $\chi_h$  is the mean horizontal susceptibility,  $\chi_h = (\chi_x + \chi_y)/2$ , then the quantity  $(\chi_h - \chi_z)/\chi_h$  corresponds roughly to the "flattening" of the susceptibility ellipsoid. Averaged over the samples of the eastern section, this quantity was found to be  $0.05 \pm .04$ . Thus the initial susceptibility is systematically smaller in the vertical direction, perpendicular to bedding.

These departures from isotropy may reflect an "error" arising during the process of deposition, one that does not need to arise from a shape anisotropy of the magnetic particles (Griffiths and others, 1960). Such a possible inclination error may contribute to the existence of an inclination that is consistently shallower than expected for the latitude of Walker Lake.

A similar calculation can be performed in the horizontal plane. The quantity  $(\chi_y - \chi_x)/\chi_h$  should reflect any strong bias for or against the north-south direction, because this direction was always within a few degrees of the y-direction of our sample cubes. Averaged over the eastern section, this quantity is  $0.04 \pm .04$ . Thus the initial susceptibility in the north-south direction appears slightly larger than that in the east-west direction.

Neither of these observations of anisotropy appears to be statistically significant. Regarding the susceptibility as spherically symmetric is adequate. In particular, the assumption of a scalar susceptibility that could legitimately be compared with the NRM, made implicitly in the previous section, was reasonable.

## SECULAR VARIATION

As a means of comparing paleomagnetic directions between the two sampled sections, we have computed virtual geomagnetic pole positions from the sample declinations and inclinations, assuming a geocentric dipole. We first "smoothed" the declination and inclination stratigraphic plots by discarding the few isolated erratic points. For these points, the standard deviations were larger in either declination or inclination than the difference between the points and linear interpolations between the two adjacent points enclosing them. Because the directions for a given horizon were generally close together, this approach seemed suitable in lieu of the more complex Fisher statistics.

Figure 12a depicts the full VGP (virtual geomagnetic pole) paths, averaging three data points for each horizon, from the eastern and western columns. Clearly, much noise obscures the path. We present these plots because they demonstrate how the data display a "far-side effect" similar to that discussed by McElhinny (1973, p. 190-191). That is, the average of the VGP positions is "over the pole" away from the sampling site. This results from a general sample inclination that is shallower than that expected from a geocentric dipole. In fact, the average inclination for our data is  $39 \pm 12$  degrees, whereas 55 degrees is expected at the sampling site for an axial geomagnetic dipole. The far-side phenomenon has been attributed to an axial dipole shifted north of the equator (Wilson, 1970, 1971), resulting in an inclination shallower than the axial dipole field in the northern hemisphere, but steeper in the southern hemisphere. However, the mean of nine regional poles lies only  $4.4^\circ$  from the geographic pole (McElhinny, 1973, p. 191), whereas the mean VGP from Walker Lake lies  $13^\circ$  from the pole. Thus, inclination error in the acquisition of detrital remanent magnetization (DRM) by sediments would seem to have played a role in producing the shallow inclinations observed at Walker Lake. The time span covered by these sediments, while not long enough to meet the dipole average requirements of Opdyke and Henry (1969) for deep sea sediments, is still very long compared with periods of

historically-observed secular variation, further suggesting that the shallowness of inclination may be related to systematic errors in the acquisition of remanence.

Figures 12b and 12c present, respectively, 5-point and 20-point running averages of data from the eastern and western columns. As others have noted (Abrahamsen and Readman, 1980; Creer and others, 1972), this reduces the amplitude of excursions, and allows one to see very large scale features that otherwise are obscured. Figure 12c in particular shows that one cannot assign a strong preference for clockwise or counterclockwise motion to these data. Indeed, it is more reasonable to describe each of the paths as "wandering."

## SUMMARY AND DISCUSSION

Detailed rock-magnetic studies on the wet sediments collected adjacent to Walker Lake, Arizona, have provided support for the conclusions of earlier workers regarding the selection of sediments suitable for paleointensity study. Investigations of the carriers of the remanance employing susceptibility, anhysteretic remanent magnetization, and saturation magnetization have revealed that the sediments did not record changes in the intensity of the ambient field during the course of deposition. While such sediments could still provide an accurate record of the direction of the geomagnetic field at the time of deposition, the lack of close agreement in magnetic direction data between the sections sampled indicates that this did not happen and that no reliable virtual geomagnetic polar path can be drawn. The paleomagnetic directions from the two sections displayed inclinations shallower than expected for an axial geomagnetic dipole resulting in far-sided, non-congruent polar paths.

## ACKNOWLEDGEMENTS

Work at Walker Lake was performed under a special use permit issued by the Forest Service, U.S. Department of Agriculture.

The authors wish to thank Ernest Gomez, Edmund Kelley, Kathleen Hogan, Steve Bressler, and Karen Chase for their assistance in the collection and processing of samples in this study.

We also wish to thank Mike Fuller for the use of the vibrating-sample magnetometer at the University of California, Santa Barbara, employed for the hysteresis measurements, and Mike Metcalf for assisting with the measurements. We thank Kenneth O'Dell for the use of a physics department magnet at Northern Arizona University, Flagstaff, for the IRM work.

## REFERENCES

- Abrahamsen, Niels, and Readman, P. W., 1980, Geomagnetic variations recorded in Older ( $\geq 23,000$  B.P.) and Younger *Yoldia* Clay ( $\sim 14,000$  B.P.) at Nørre Lyngby, Denmark: *Geophysical Journal of the Royal Astronomical Society*, v. 62, p. 329-344.
- Adam, D. P., Hevly, R. H., and Diggs, R. E., 1985, Pollen data from a 2.93-meter Holocene lacustrine section from Walker Lake, Coconino County, Arizona: U.S. Geological Survey Open-File Report 85-46, 20 p.
- Banerjee, S. K., King, J., and Marvin, J., 1981, A rapid method for magnetic granulometry with applications to environmental studies: *Geophysical Research Letters*, v. 8, p. 333-336.
- Berry, R. W., McCormick, C. W., and Adam, D. P., 1982, Pollen data from a 5-meter upper Pleistocene lacustrine section from Walker Lake, Coconino County, Arizona: U.S. Geological Survey Open-File Report 82-383, 107 p.
- Creer, K. M., Thompson, R., and Molyneux, L., 1972, Geomagnetic secular variation recorded in the stable magnetic remanence of recent sediments: *Earth and Planetary Science Letters*, v. 14, p. 115-127.
- Dankers, P., 1978, Magnetic properties of dispersed natural iron-oxides of known grain-size: Utrecht, Netherlands, University of Utrecht, Ph.D. thesis, p.
- Day, R., Fuller, M. D., and Schmidt, V. A., 1977, Hysteresis properties of titanomagnetites: grain size and composition dependence: *Physics of Earth and Planetary Interiors*, v. 13, p. 260-266.
- Griffiths, D. H., King, R. F., Rees, A. I., and Wright, A. E., 1960, The remanent magnetism of some recent varved sediments: *Proceedings of the Royal Society, Series A*, v. 256, p. 359-383.
- Harrison, C. G. A., 1966, The paleomagnetism of deep-sea sediments: *Journal of Geophysical Research*, v. 71, p. 3033-3043.
- Johnson, E. A., Murphy, T., and Torreson, O. W., 1948, Pre-history of the Earth's magnetic field: *Terrestrial Magnetism and Atmospheric Electricity*, v. 53, p. 349-372.

- Johnson, H. P., Kinoshita, H., and Merrill, R. T., 1975, Rock magnetism and paleomagnetism of some north Pacific deep-sea sediment cores: Geological Society of America Bulletin, v. 86, p. 412-420.
- King, J., Banerjee, S. K., Marvin, J., and Özdemir, O., 1982, A comparison of different magnetic methods for determining the relative grain size of magnetite in natural materials: some results from lake sediments: Earth and Planetary Science Letters, v. 42, p. 404-419.
- King, J., Banerjee, S. K., and Marvin, J., 1983, A new rock-magnetic approach to selecting sediments for geomagnetic paleointensity studies: application to paleointensity for the last 4000 years: Journal of Geophysical Research, v. 88, p. 5911-5921.
- Levi, S., and Banerjee, S. K., 1976, On the possibility of obtaining relative paleointensities from lake sediments: Earth and Planetary Science Letters, v. 29, p. 219-226.
- McElhinny, M. W., 1973, Palaeomagnetism and Plate Tectonics: London, England, Publication Syndics of the Cambridge University Press, 358 p.
- Nakajima, Tadashi, and Kawai, Naoto, 1973, Secular variation in the recent 60,000 years found from the Lake Biwa sediments: Rock Magnetism and Paleogeophysics, (Research Group, Japan), v. 1, p. 34-38.
- Nesbitt, J. D., 1966, Variation of the ratio intensity to susceptibility in red sandstones: Nature, v. 210, p. 618.
- Opdyke, N. D., and Henry, K. W., 1969, A test of the dipole hypothesis: Earth and Planetary Science Letters, v. 6, p. 139-151.
- Özdemir, O., and Banerjee, S. K., 1982, A preliminary magnetic study of soil evolution in west central Minnesota: Earth and Planetary Science Letters, v. 59, p. 393-403.
- Robinson, H. H., 1913, The San Francisco Volcanic Field: U.S. Geological Survey Professional Paper 76, 213 p.
- Thellier, E., and Thellier, O., 1959, Sur l'intensite du champ magnetique terrestre dan le passe historique et geologique: Annals of Geophysics, v. 15, p. 285-376.

Verbeck, K. J., 1971, The mechanism of emplacement of the Marble Mountain (White Horse Hills) Laccolith: Pennsylvania State University, M.S. Thesis, 112 p.

Wilson, R. L., 1970, Permanent aspect of the earth's non-dipole magnetic field over Upper Tertiary times: *Geophysical Journal of the Royal Astronomical Society*, v. 19, p. 417-437.

Wilson, R. L., 1971, Dipole offset — the time averaged palaeomagnetic field over the past 25 million years: *Geophysical Journal of the Royal Astronomical Society*, v. 22, p. 491-504.

## FIGURE CAPTIONS

Figure 1. Map showing location of Walker Lake, Coconino County, Arizona.

Figure 2. Sketch of pit adjacent to Walker Lake showing generalized stratigraphy and distribution of channel sample monoliths,  $^{14}\text{C}$  sampling sites, and samples for x-ray photography (dashed outlines). Channels analyzed for paleomagnetism are hatched; unpatterned channels are archived.

Figure 3. Generalized columnar section and  $^{14}\text{C}$  chronology of the Walker Lake sediments. Units A, B, C, and D are lake beds consisting of laminated and massive clay. Units A-C are finely laminated; unit D is coarsely laminated. Granular intervals suggesting periods of dessication are indicated by slashes. Preliminary radiocarbon dates are from Stephen W. Robinson (personal communication, 1984).

Figure 4. Isothermal remanent magnetization (IRM) acquisition curves for five samples from the Walker Lake sediments. Stratigraphic depths in meters are as indicated. Samples are from the east section.

Figure 5. Orthogonal demagnetization diagrams for four samples from the Walker Lake sediments, east section. Stratigraphic depths in meters are as indicated.

Figure 6. Magnetic stratigraphy in the Walker Lake sediments: 6A - east section; 6B - west section. Magnetic declination, inclination, volume magnetization, and initial susceptibility are plotted as functions of stratigraphic position. Most horizons have three dots, indicating measurement of three samples. Directions and intensities are after partial AF demagnetization at 7.5 mT.

Figure 7. Plot of anhysteretic remanent magnetization (ARM) acquired in a steady field of 0.04 mT vs initial susceptibility for all samples from the east section in Walker Lake. Regions of relative variations in grain size, as discussed by Banerjee and others (1981) and King and others (1982), are indicated.

Figure 8. Plot of hysteresis parameters, as discussed by Day and others (1977), for 17 samples from the Walker Lake sediments. The dotted lines enclose the area suggested by King and others (1983) as defining sediments likely to be suitable for paleointensity work; dashed lines indicate pseudo-single domain region of Day and others (1977);  $J_S$ --saturation magnetization;  $J_{RS}$ --saturation isothermal remanence;  $H_C$ --coercive force;  $H_{RC}$ --coercivity of remanence. See Figure 7 for explanation of plotted symbols.

Figure 9. Normalized alternating-field demagnetization curves for two samples from Walker Lake. For each sample, demagnetization of the original NRM and imposed ARM and IRM are shown. a) coarser, b) finer magnetite grain-size fractions.

Figure 10. (a) Plots of the ratio  $NRM/ARM$  vs AF demagnetization level for several samples from Walker Lake. (b) Plots of the ratio  $NRM/IRM$  for the same samples. Note that no curves are particularly "flat" over any appreciable range of demagnetization level, implying that neither ARM nor IRM is likely to be useful as a paleointensity indicator.

Figure 11. Plot of NRM vs initial susceptibility for all samples from the east section in Walker Lake. Note the strong correlation, indicating that the NRM does not reflect variation in the intensity of the field at the time of deposition. Compare, also, the intensity and susceptibility columns in Figure 6.

Figure 12. a). Secular variation path for the east and west sections in Walker Lake. Note the clustering of virtual geomagnetic poles "over the pole" from the sampling site. b). Five-point (10 cm of section) running average of the data. c). Twenty-point (40 cm of section) running average of the data. Azimuthal equidistant projection.

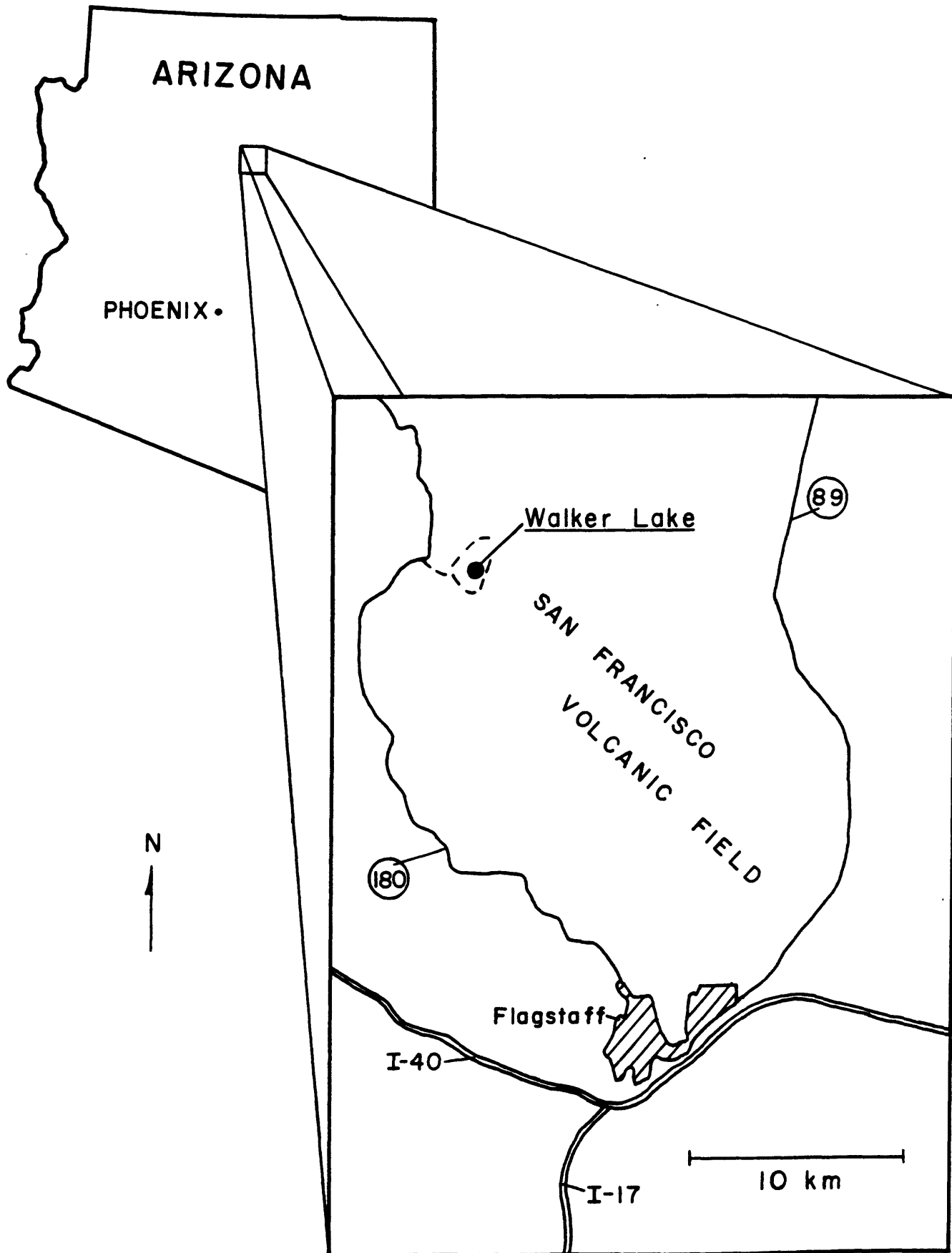


Figure 1. Map showing location of Walker Lake, Coconino County, Arizona.

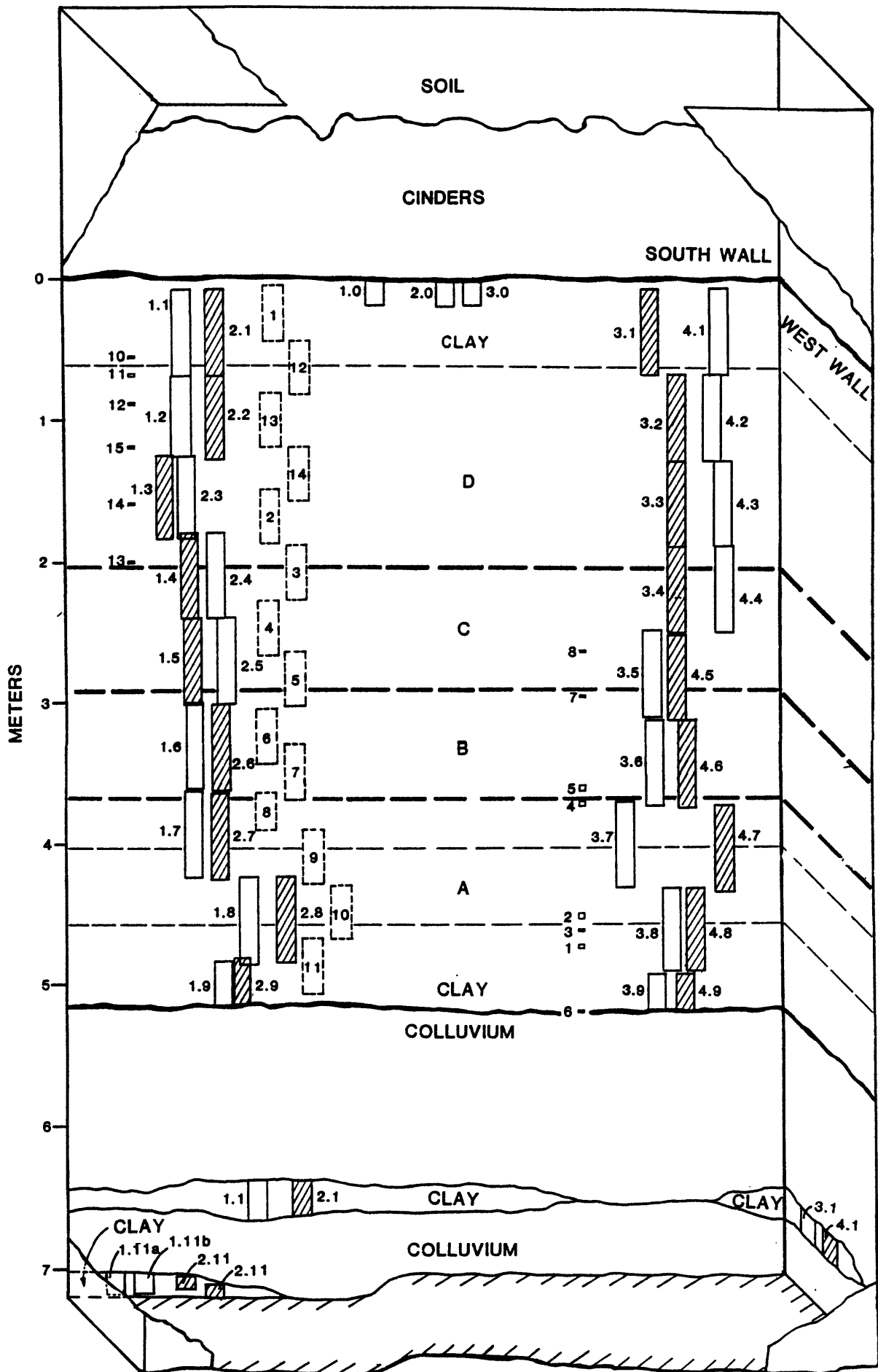


Figure 2. Sketch of pit adjacent to Walker Lake showing generalized stratigraphy and distribution of channel sample monoliths, <sup>14</sup>C sampling sites, and samples for x-ray photography (dashed outlines). Channels analyzed for paleomagnetism are hatched; unpatterned channels are archived.

DEPTH  
IN METERS

UNIT THICKNESS  
IN METERS

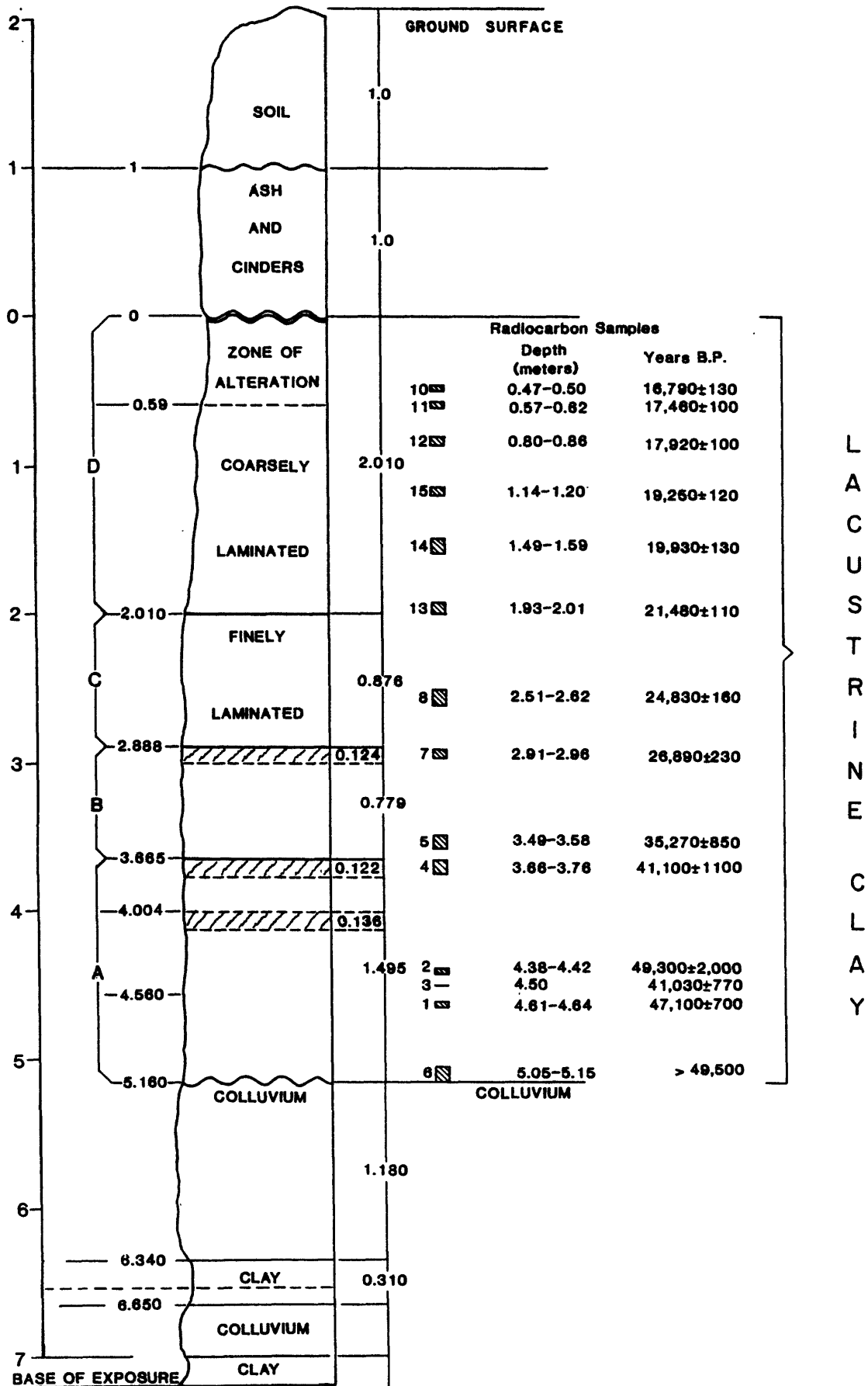


Figure 3. Generalized columnar section and <sup>14</sup>C chronology of the Walker Lake sediments. Units A, B, C, and D are lake beds consisting of laminated and massive clay. Units A-C are finely laminated; unit D is coarsely laminated. Granular intervals suggesting periods of dessication are indicated by slashes. Preliminary radiocarbon dates are from Stephen W. Robinson (personal communication, 1984).

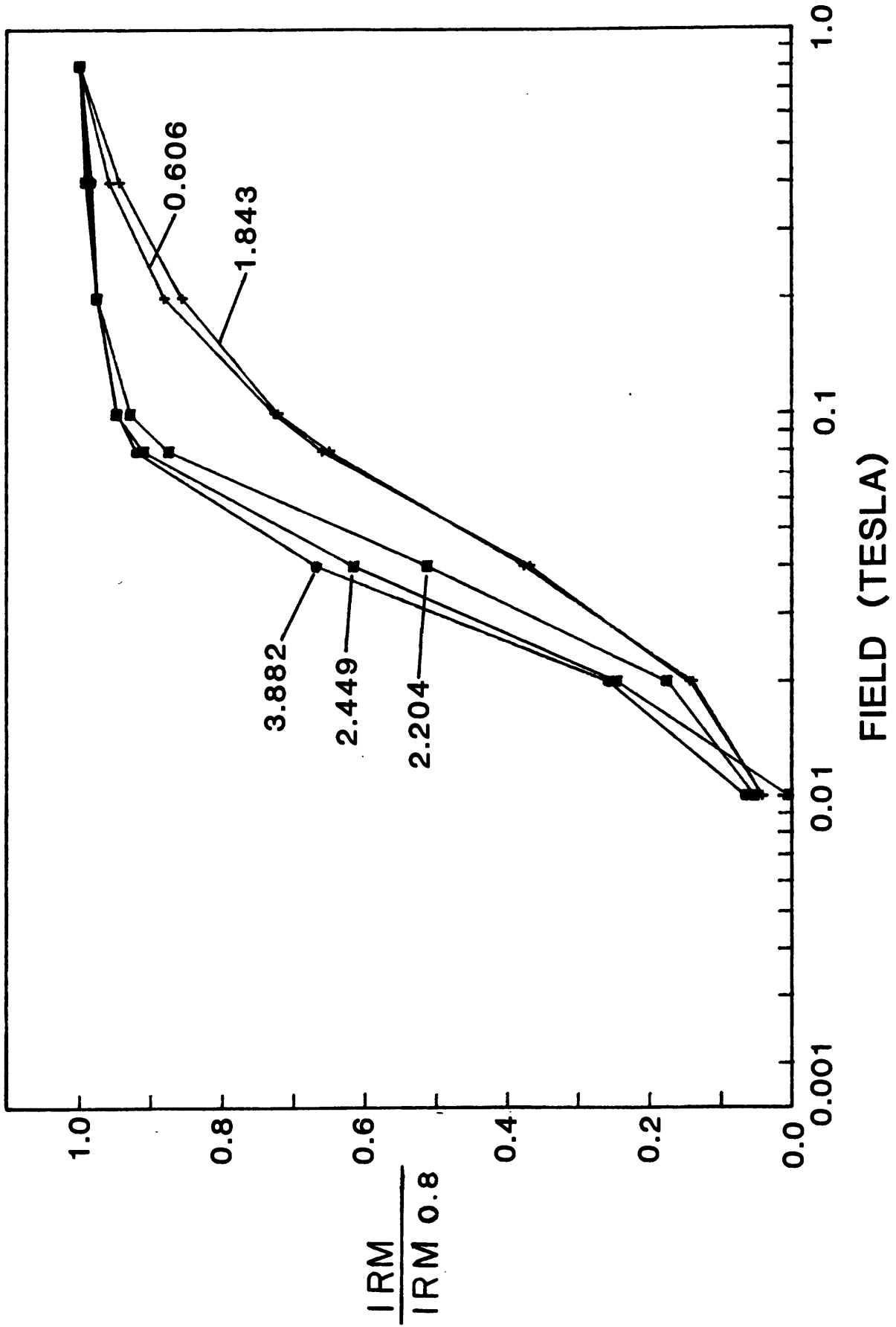
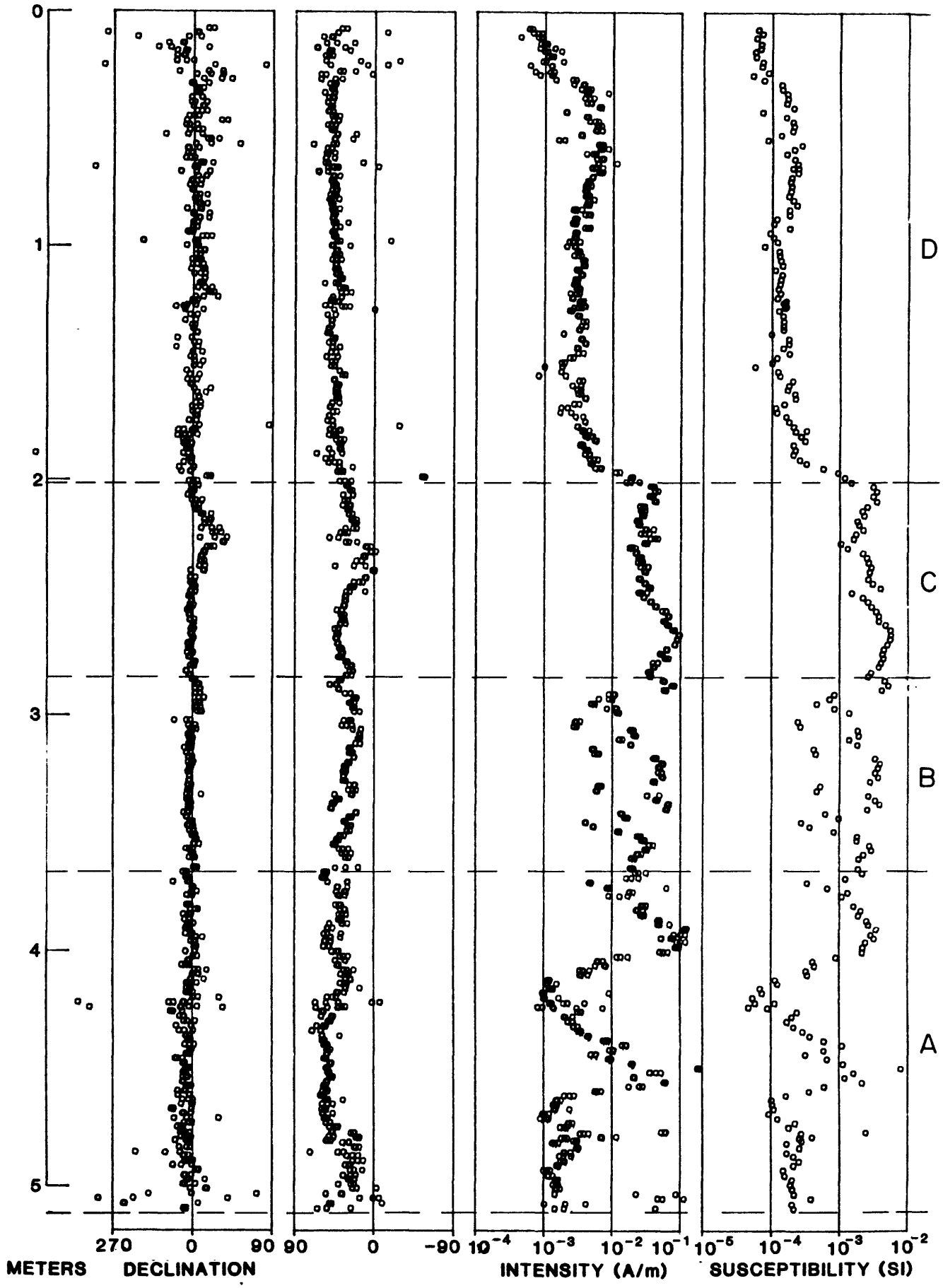


Figure 4. Isothermal remanent magnetization (IRM) acquisition curves for five samples from the Walker Lake sediments. Stratigraphic depths in meters are as indicated. Samples are from the east section.





**WALKER LAKE, EAST**

Figure 6. Magnetic stratigraphy in the Walker Lake sediments: 6A - east section; 6B - west section. Magnetic declination, inclination, volume magnetization, and initial susceptibility are plotted as functions of stratigraphic position. Most horizons have three dots, indicating measurement of three samples. Directions and intensities are after partial AF demagnetization at 7.5 mT.

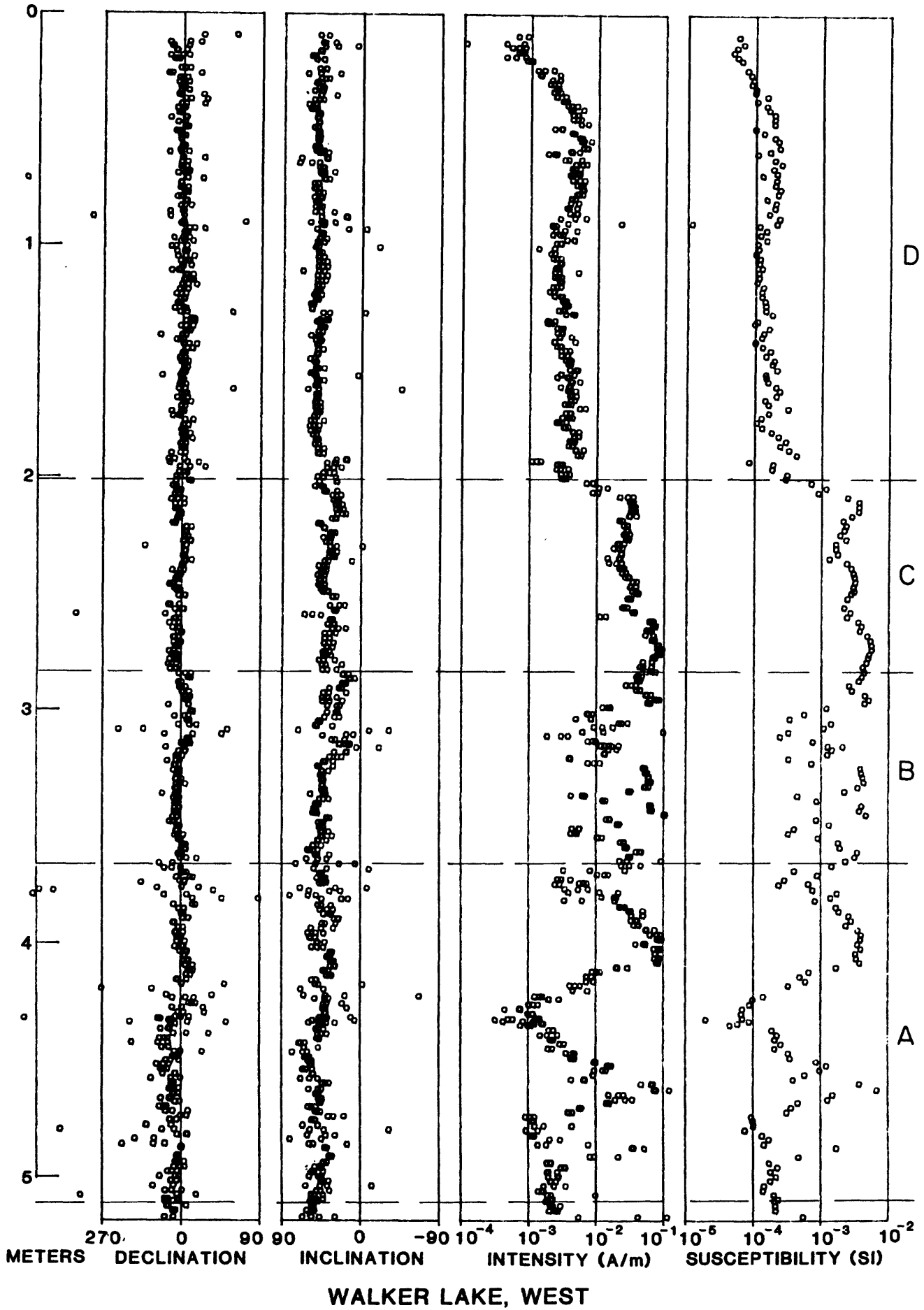


Figure 6B - west section.

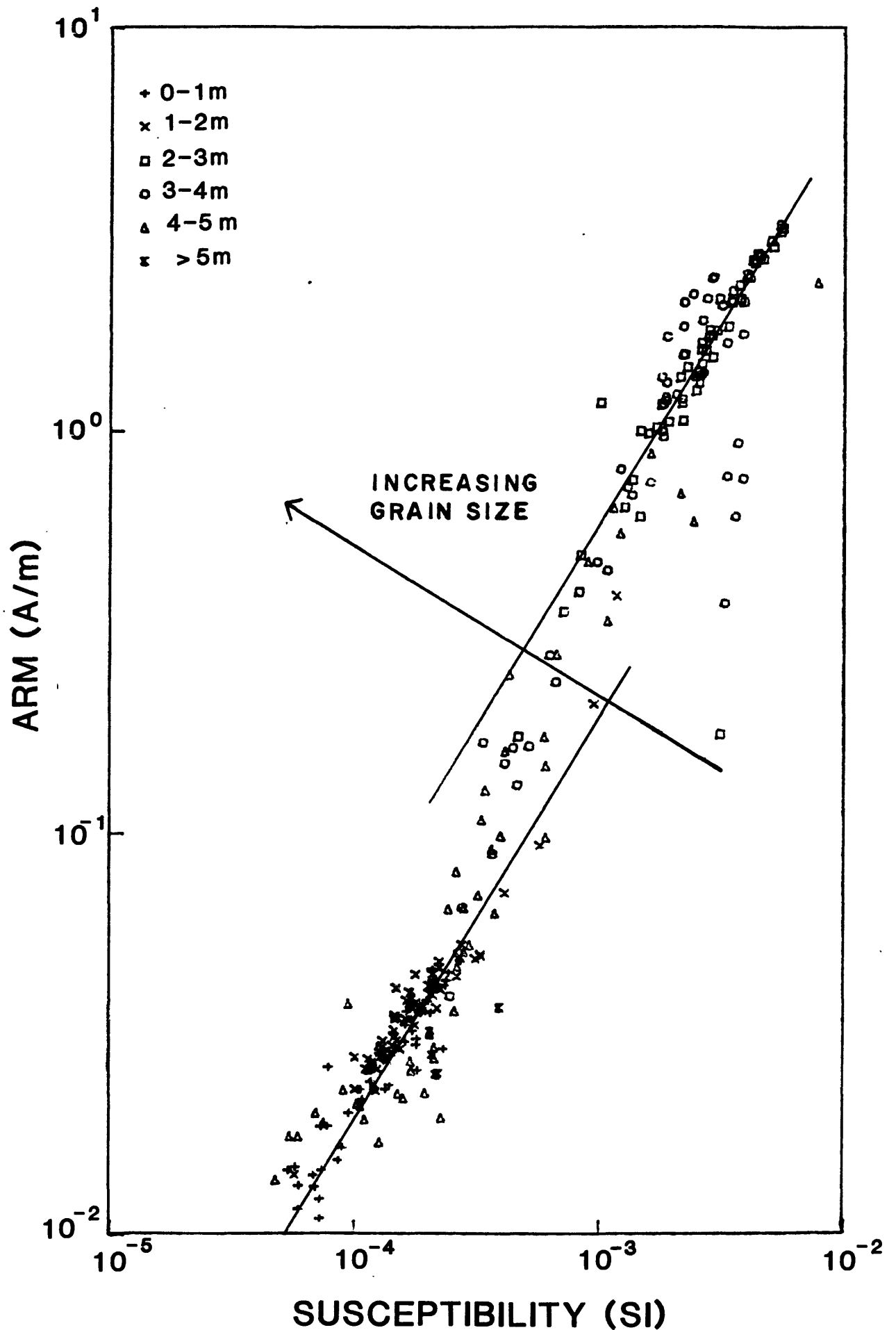


Figure 7. Plot of anhysteretic remanent magnetization (ARM) acquired in a steady field of 0.04 mT vs initial susceptibility for all samples from the east section in Walker Lake. Regions of relative variations in grain size, as discussed by Banerjee and others (1981) and King and others (1982) are indicated.

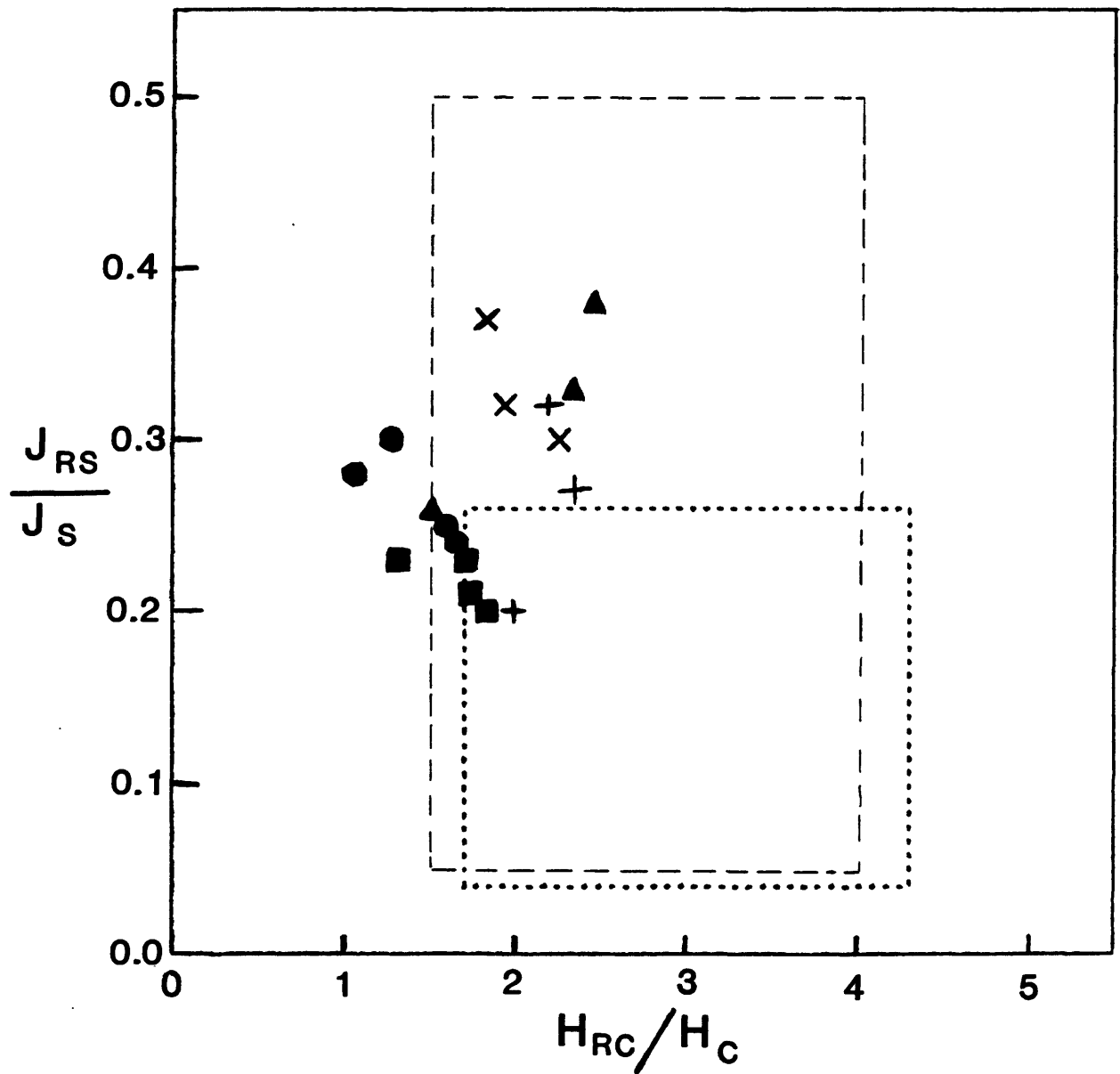


Figure 8. Plot of hysteresis parameters, as discussed by Day and others (1977), for 17 samples from the Walker Lake sediments. The dotted lines enclose the area suggested by King and others (1983) as defining sediments likely to be suitable for paleointensity work; dashed lines indicate pseudo-single domain region of Day and others (1977);  $J_S$ --saturation magnetization;  $J_{RS}$ --saturation isothermal remanence;  $H_C$ --coercive force;  $H_{RC}$ --coercivity of remanence. See Figure 7 for explanation of plotted symbols.

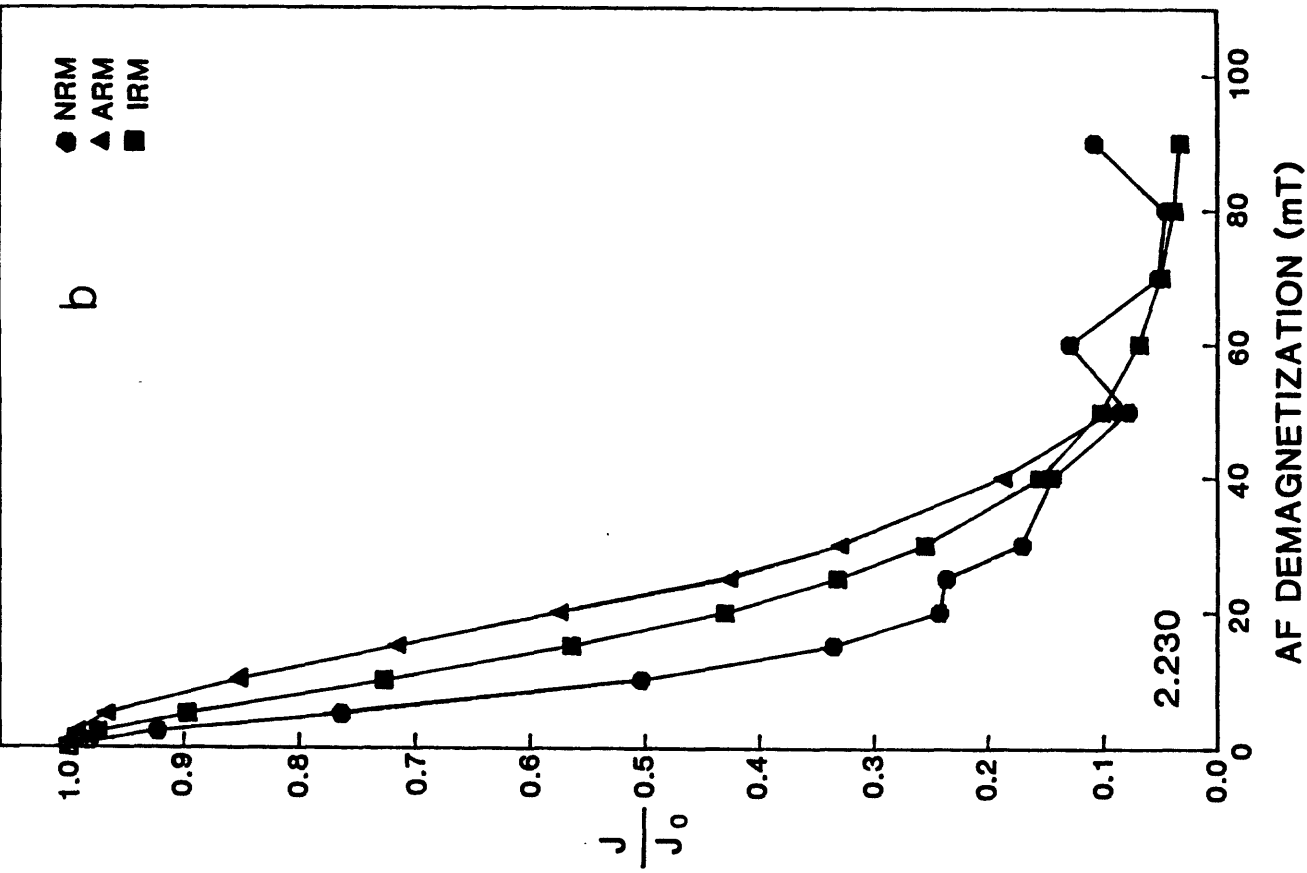
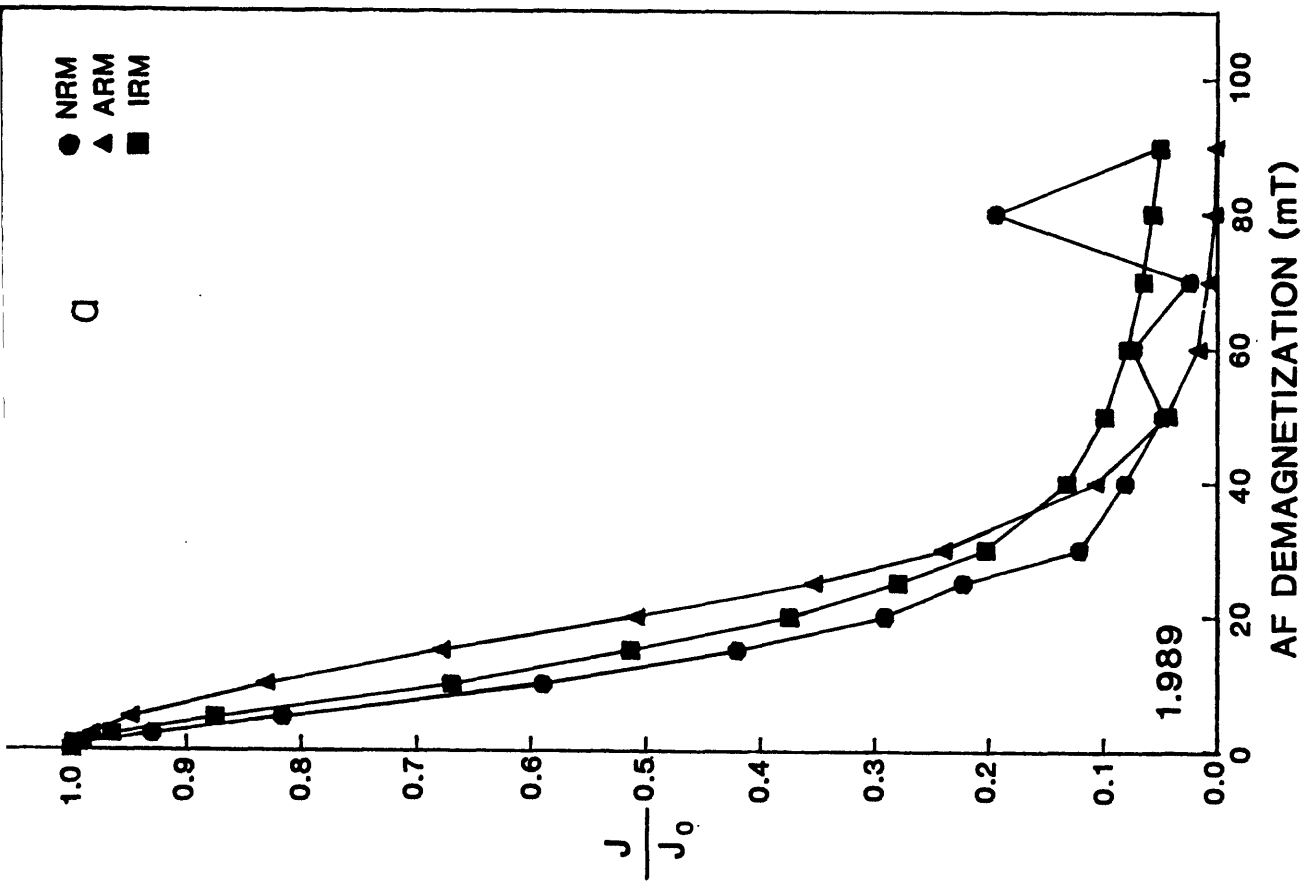


Figure 9. Normalized alternating-field demagnetization curves for two samples from Walker Lake. For each sample, demagnetization of the original NRM and imposed ARM and IRM are shown. a) coarser, b) finer magnetite grain-size fractions.

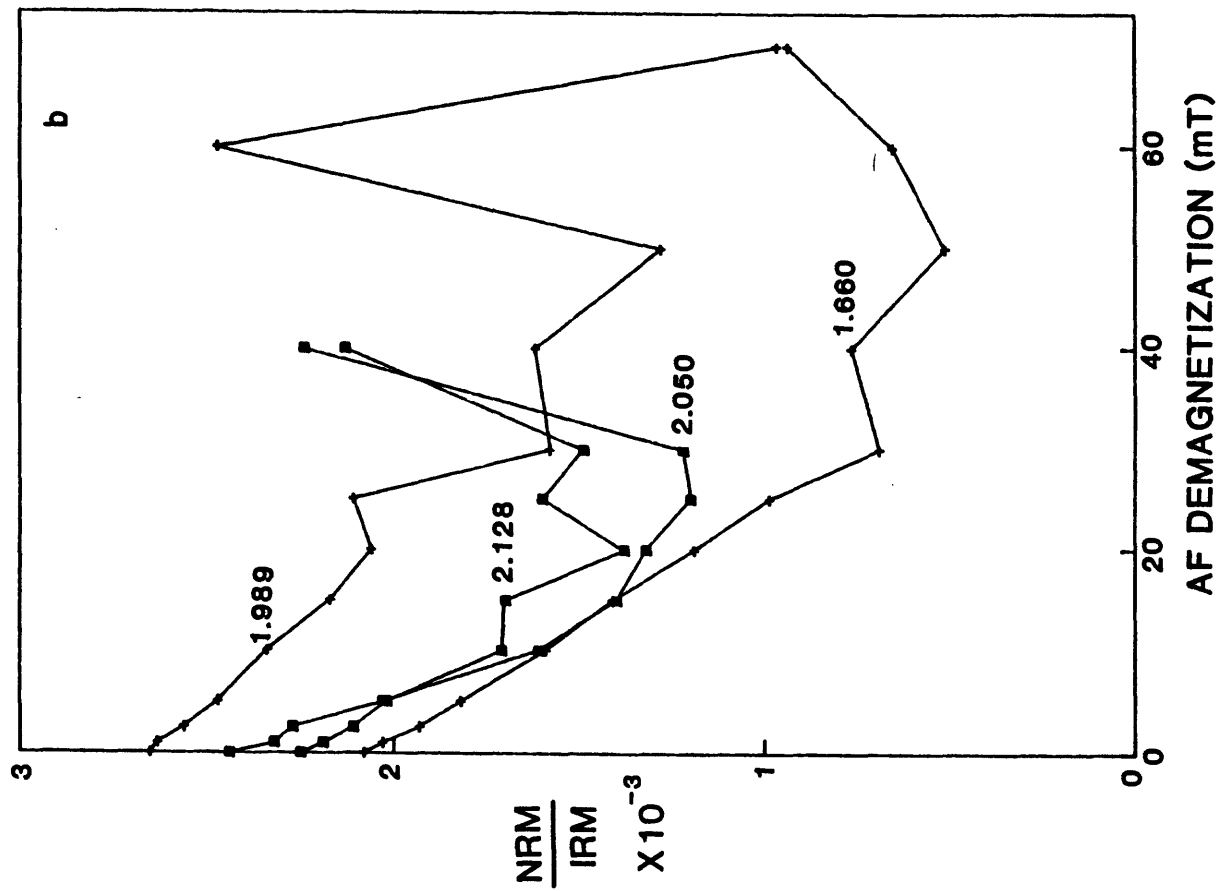
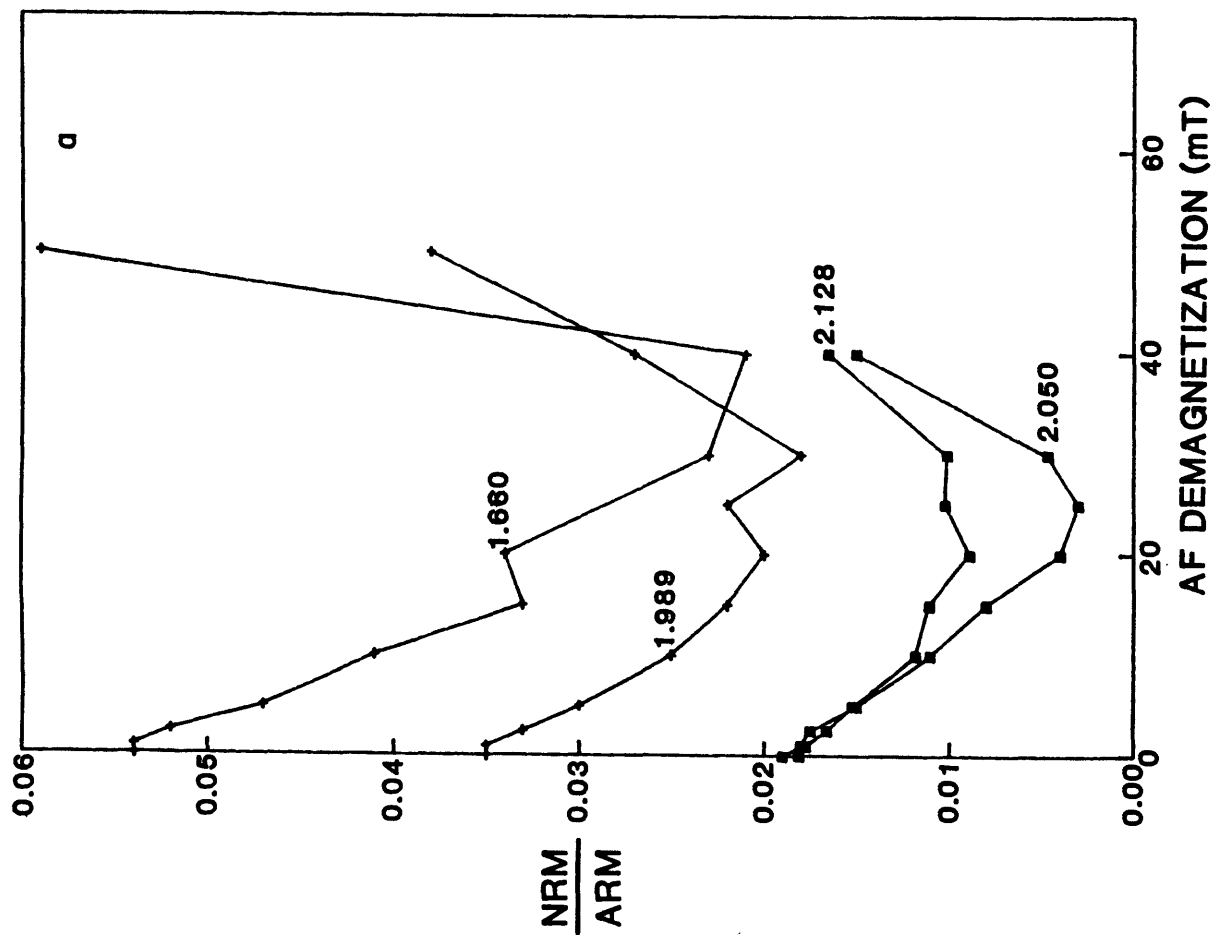


Figure 10. (a) Plots of the ratio NRM/ARM vs AF demagnetization level for several samples from Walker Lake. (b) Plots of the ratio NRM/IRM for the same samples. Note that no curves are particularly "flat" over any appreciable range of demagnetization level, implying that neither ARM nor IRM is likely to be useful as a paleointensity indicator.

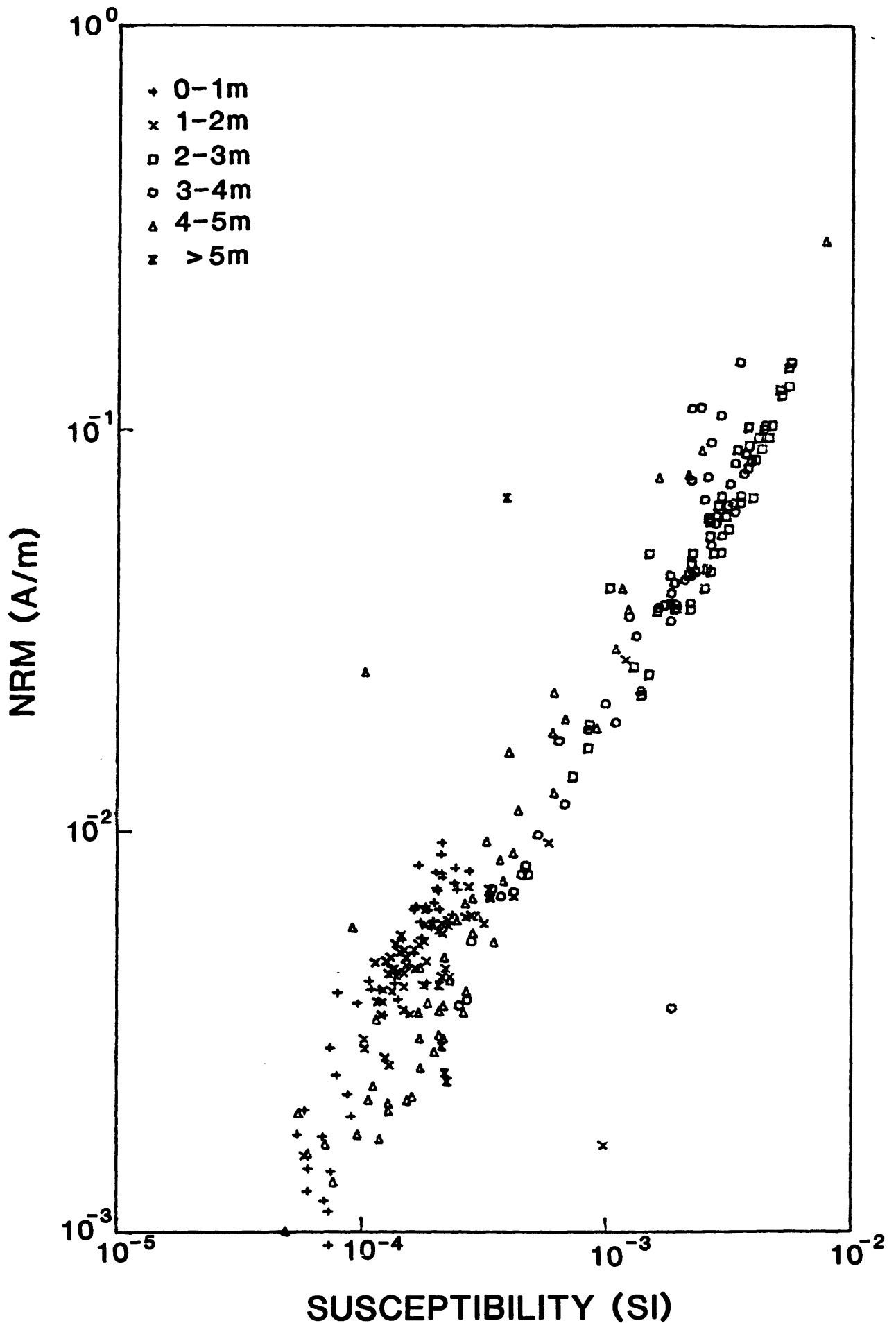


Figure 11. Plot of NRM vs initial susceptibility for all samples from the east section in Walker Lake. Note the strong correlation, indicating that the NRM does not reflect variation in the intensity of the field at the time of deposition. Compare, also, the intensity and susceptibility columns in Figure 6.

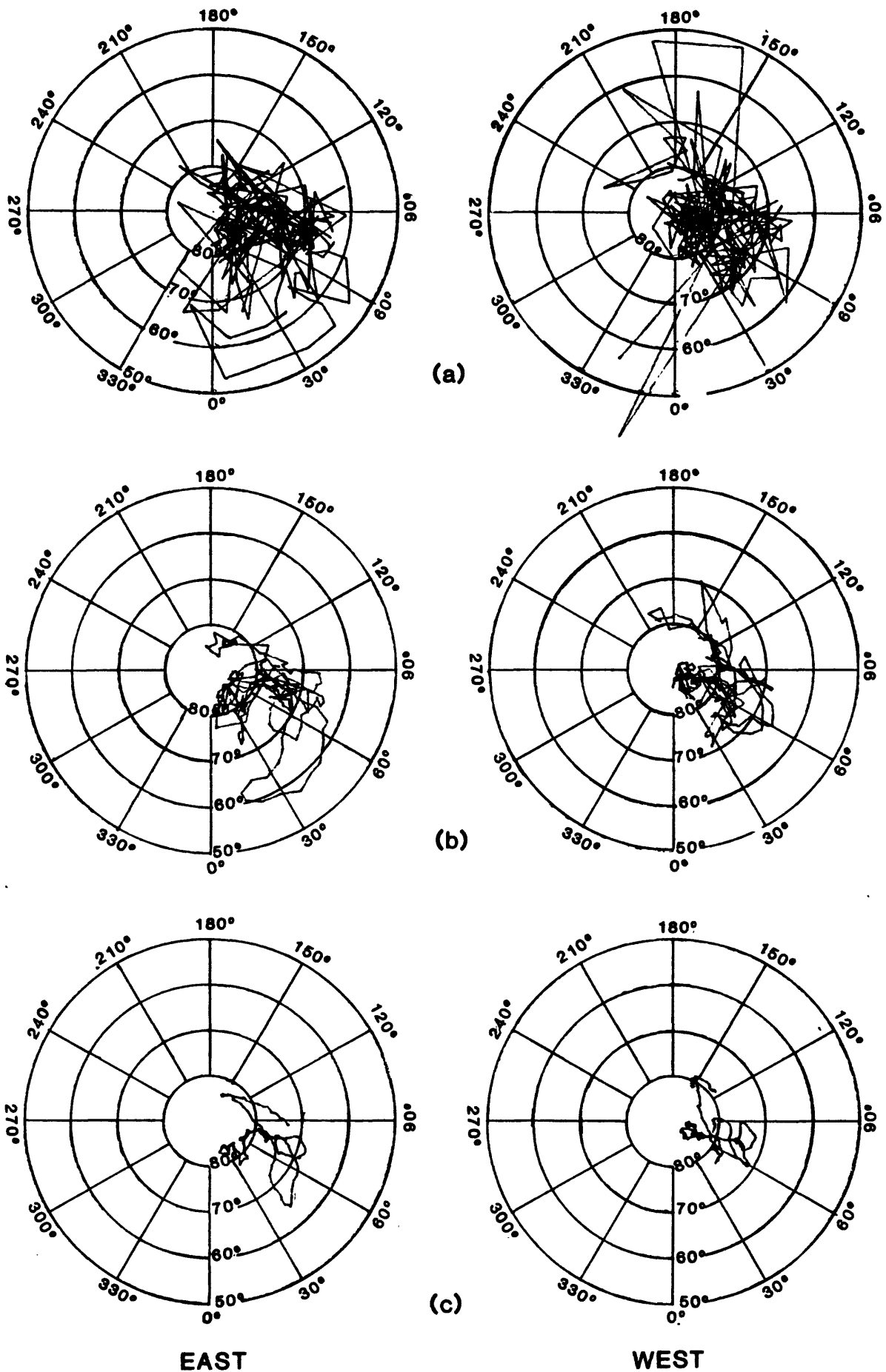


Figure 12. a). Secular variation path for the east and west sections in Walker Lake. Note the clustering of virtual geomagnetic poles "over the pole" from the sampling site. b). Five-point (10 cm of section) running average of the data. c). Twenty-point (40 cm of section) running average of the data. Azimuthal equidistant projection.